

Published in final edited form as:

Cancer Res. 2011 October 1; 71(19): 6153–6164. doi:10.1158/0008-5472.CAN-11-0720.

Proto-oncogene PBF/PTTG1IP regulates thyroid cell growth and represses radioiodide treatment

Martin L. Read¹, Greg D. Lewy¹, Jim C.W. Fong¹, Neil Sharma¹, Robert I. Seed¹, Vicki E. Smith¹, Erica Gentilin², Adrian Warfield³, Margaret C. Eggo¹, Jeffrey A. Knauf⁴, Wendy E. Leadbeater¹, John C. Watkinson³, Jayne A. Franklyn¹, Kristien Boelaert¹, and Christopher J. McCabe¹

¹School of Clinical and Experimental Medicine, Institute of Biomedical Research, University of Birmingham, B15 2TH, UK

²Section of Endocrinology, Department of Biomedical Sciences and Advanced Therapies, University of Ferrara, Via Savonarola 9, 44121 Ferrara, Italy

³University Hospitals Birmingham NHS Foundation Trust, Birmingham, B15 2TJ, UK

⁴Memorial Sloan-Kettering Cancer Center, New York, NY 10021, USA

Abstract

PTTG Binding Factor (PBF or PTTG1IP) is a little characterised proto-oncogene that has been implicated in the etiology of breast and thyroid tumors. In this study, we created a murine transgenic model to target PBF expression to the thyroid gland (PBF-Tg mice) and found that these mice exhibited normal thyroid function but a striking enlargement of the thyroid gland associated with hyperplastic and macrofollicular lesions. Expression of the sodium iodide symporter (NIS), a gene essential to the radioiodine ablation of thyroid hyperplasia, neoplasia and metastasis, was also potently inhibited in PBF-Tg mice. Critically, iodide uptake was repressed in primary thyroid cultures from PBF-Tg mice, which could be rescued by PBF depletion. PBF-Tg thyroids exhibited upregulation of Akt and the TSH receptor (TSHR), each known regulators of thyrocyte proliferation, along with upregulation of the downstream proliferative marker cyclin D1. We extended and confirmed findings from the mouse model by examining PBF expression in human multinodular goitres (MNG), a hyperproliferative thyroid disorder, where PBF and TSHR was strongly upregulated relative to normal thyroid tissue. Further, we showed that depleting PBF in human primary thyrocytes was sufficient to increase radioiodine uptake. Together, our findings indicate that overexpression of PBF causes thyroid cell proliferation, macrofollicular lesions and hyperplasia, as well as repression of the critical therapeutic route for radioiodide uptake.

Keywords

radioiodine; NIS; hyperplasia; Akt; thyroid cancer

Corresponding author: Professor Christopher J McCabe, Professor of Molecular Endocrinology, School of Clinical and Experimental Medicine, Institute of Biomedical Research, University of Birmingham, Birmingham, B15 2TH, UK. Tel: 44 121 415 8713; Fax: 44 121 415 8712; mccabcjz@bham.ac.uk.

Precis This study of a little characterized proto-oncogene in thyroid hyperplasia and neoplasia reveals that it functions in blocking the chief route of radioiodine uptake which is vital for clinical treatment of thyroid cancer.

Introduction

Described in only eleven publications (1-11) Pituitary Tumor Transforming Gene binding factor (PBF) was identified through its ability to interact with PTTG1, the human securin (3). *PBF* comprises 6 exons spanning 24 Kb within chromosomal region 21q22.3. The 180 amino acid peptide sequence of PBF shares no significant homology with other human proteins, but is highly conserved across a wide diversity of animal species (73% homology to mouse, 67% frog, 60% chicken, 52% zebra fish), suggesting both unique function and significant evolutionary importance. *PBF* is widely expressed in normal human tissues, including normal thyroid (3, 10). Whilst expression is low in normal breast tissue, immunohistochemical analysis demonstrated that PBF was strongly expressed in epithelial cells of all types and grades of breast tumour assessed (11).

Initial protein prediction studies suggested that PBF was a cell surface glycoprotein due to a potential N-terminal signal peptide, transmembrane domain, endocytosis motif and two putative N-glycosylation sites (10). PBF also possesses an extracellular N-terminal cysteine-rich region, similar to that found in the membrane-associated plexins, semaphorins and integrins (12). In contrast to evidence supporting the characterisation of PBF as a membrane protein, the presence of a bipartite nuclear localisation signal (NLS) near the C-terminus suggested PBF may also be a nuclear protein (3).

We previously characterised PBF expression in thyroid cancers, and demonstrated it to be a transforming gene *in vitro*, and to be tumourigenic *in vivo* (8). Furthermore, high PBF expression was independently associated with poor prognosis in human differentiated thyroid cancer. Most recently, we showed that PBF represses iodide uptake in thyroid cells *in vitro*, both through transcriptional regulation (2) and altered subcellular trafficking (6) of the sodium iodide symporter (NIS). Outside the thyroid, we recently described a role for PBF in the aetiology of breast cancer (11), and defined PBF function in a mouse model of Down's Syndrome angiogenesis (5).

PBF is thus a relatively uncharacterised protein implicated in multiple cellular processes, particularly in the setting of endocrine neoplasia. However, the precise function of PBF *in vivo*, and the oncogenic potential of PBF within a specific organ, has not been tested. Whilst subcutaneous injection of stable NIH3T3 lines over-expressing PBF elicited large and aggressive tumours in nude mice (8), a more physiological appraisal of tumour induction is lacking. Thus, to investigate the function of PBF *in vivo*, we generated a murine transgenic model of PBF expression (PBF-Tg) targeted to the thyroid gland. We now present extensive data suggesting that PBF regulates thyroid gland growth through increased cell proliferation, an effect that is independent of thyroid function and growth factor induction, and induces significant hyperplasia. Furthermore, we propose that PBF represents a gene of direct clinical relevance to thyroid hyperplasia and neoplasia, given that it is over-expressed in human MNG and potently represses iodide uptake *in vivo*.

Methods

Generation of PBF-Tg transgenic mice

WT and transgenic PBF-Tg mice were bred at the University of Birmingham and all experiments performed in accordance with U.K. Home Office regulations. The generation of the PBF-Tg transgenic line was performed by microinjection of fertilized mouse oocytes with the Tg-PBF-HA transgene and subsequent transfer into pseudopregnant females, as per standard protocols (13-14). Further details on construction of the Tg-PBF-HA transgene are provided in Supplementary Fig. S1.

Transgene copy number was determined by real-time RT-PCR essentially as described previously (15). Primers used to detect the human PBF gene were 5'-GCTTGTCTGGACTACCCAGTTACA-3' (forward), 5'-AGCGTGCAGAGCTCAATTTACA-3' (reverse) and 5'-FAMCGTCTTGCCACCGGCTTCCCT-3' (probe). To normalise DNA in PCR reactions we used primers 5'-CAGAAAACCATGAGAGGCAATG-3' (forward), 5'-TTCTCCCATGAGACGACAGTGA-3' (reverse) and 5'-VICTTCAAGTGCATTATCCCCTCCTCGGTG-3' (probe) directed to a 89 bp sequence in the *DSCAM* gene, which is conserved between mouse and human genomes.

RNA extraction, reverse transcription quantitative PCR and Western blot analysis

Total RNA was extracted from mouse thyroids using the RNeasy Micro Kit (Qiagen) and reverse transcribed using the Reverse Transcription System (Promega), as previously described (2). Expression of specific mRNAs was determined using 7500 Real-time PCR system (Applied Biosystems; ref (16)). Western blot analysis was performed as we have described previously (1, 6, 17). After blocking Western gels were probed with specific antibodies against TSHR (H-155), (Santa Cruz Biotechnology), 1:500; TSHR (2C11), (AbD Serotec), 1:200; phospho-Akt (Ser473) (D9E) XP (Cell Signalling Technology), 1:1000; total Akt, (Millipore), 1:1000 and PBF (6, 11), 1:1000.

Immunohistochemistry

Mouse thyroid specimens were immunostained with specific antibodies against cyclin D1, (Abcam), 1:100; HA, (Covance Research Products), 1:1000 and NIS, (Alpha Diagnostic Intl), 1:50 using protocols as described previously (8, 18). Immunostained sections were counterstained with Mayer's hematoxylin. For negative controls the primary antibody was replaced by 10% normal goat serum.

Analysis of thyroid morphology

Thyroid glands were removed from mice aged between 4 and 78 weeks using a dissecting microscope. H&E and immunostained thyroid tissue sections were viewed under a light-microscope (Zeiss) and images captured using Axiovision software (Version 4). The diameter of thyroid follicles (major axis) was measured using ImageJ software. A standard 100 μm scale bar (Axiovision) was used to convert pixels to μm .

Primary thyrocyte culture, siRNA transfection and iodide uptake assays

Primary thyrocyte cultures were performed as described previously (17, 19). Seven days after seeding thyrocyte cultures were transfected with PBF-specific and control siRNA (Ambion) by lipofectamine-2000 (Invitrogen) using standard protocols. 72 hours post-transfection, iodide (^{125}I) uptake assays were performed to assess NIS function as described previously (6). Relative iodide uptake was corrected for protein concentration as measured by the Bradford assay.

Thyroid function tests

Total T_4 and total T_3 in serum of WT and PBF-Tg mice were measured after centrifugation of clotted blood samples using RIA kits (MP Biomedicals). Mouse serum TSH concentrations were determined by the laboratory of Prof Samuel Refetoff (University of Chicago, USA). Details of this assay have been published (20).

Human thyroid samples

Collection of thyroid samples was in accordance with approval of the Local Research Ethics committee, and subjects gave informed written consent. Normal thyroid was obtained from the contralateral lobe at the time of surgery.

Statistics

Data are displayed as mean \pm SEM. All statistical tests were performed with the 2-tailed Student's *t*-test, unless otherwise indicated. *P* values < 0.05 were considered significant.

Results

A murine model of thyroid-targeted PBF induction

To investigate the physiological effect of enhanced PBF expression within thyroid follicular epithelial cells, we constructed a FVB/N transgenic line with targeted expression of PBF driven by the bovine thyroglobulin promoter (Fig. 1A). Real-time PCR-based zygosity assays indicated that a single copy of the Tg-PBF-HA transgene had integrated into the genomic DNA of the founder mouse and in G1 hemizygotes (Supplementary Fig. S2). Quantification of PBF transgene expression in PBF-Tg thyroids showed an ~7-fold increase relative to endogenous PBF protein levels in wild-type (WT) thyroids (Fig. 1B). There was no significant expression of the PBF transgene in other major organs examined, including the liver, kidney and spleen (Supplementary Fig. S3). Immunohistochemistry using an anti-HA antibody revealed intense brown staining of the HA-tagged transgene in thyroid follicular epithelial cells, where it was predominantly localised within the cytoplasm (Fig. 1C).

Male PBF-Tg mice showed no significant change in body weight compared with WT littermates up to 10 weeks (Fig. 1D). In contrast, there was a slight increase in body weight of female PBF-Tg mice at both 7 (13.4% weight gain, $P < 0.0001$) and 10 (5.5% weight gain, $P = 0.04$) weeks of age compared to female WT mice. Survival was non-significantly decreased in PBF-Tg mice (Fig. 1E, $14 \pm 5\%$ decrease compared with WT by 18 months of age, $P = 0.127$). No consistent cause of death was identified in those PBF-Tg mice which died earlier than WT.

PBF-Tg mice show enlarged thyroid glands and altered follicular structure

The most striking phenotype of PBF-Tg mice was an increase in thyroid size and weight. PBF-Tg thyroid glands were 1.7-fold heavier than those of WT litter-mates by 6-7 weeks, and up to 3.2 times heavier by 52 weeks (Fig. 2A and Supplementary Fig. S4). At 52 weeks of age, the mean thyroid weight of PBF-Tg mice was 10.0 ± 0.6 mg compared with 3.26 ± 0.13 mg for WT mice. Increased thyroid size persisted to 78 weeks (Fig. 2A). Interestingly, thyroid glands from female PBF-Tg mice were significantly larger than those of male PBF-Tg littermates at 52 weeks of age (38.5% weight difference, $P = 0.0045$, Supplementary Fig. S4C). Critically, the penetrance of increased thyroid weight in PBF-Tg mice was 100%, with all transgenic mice demonstrating markedly enlarged thyroid glands ($n = 213$). In addition, the thyroid glands of transgenic mice had a superficially nodular appearance on macroscopic evaluation (Fig. 2B).

To examine mouse thyroid glands microscopically, we performed H&E staining on sections from PBF-Tg and WT mice. Composite images of complete thyroid lobes from PBF-Tg and WT mice demonstrated that the increased size of PBF-Tg thyroids (3-4 mm compared with 2 mm overall length, respectively, Fig. 2C) might be due to an increased follicular diameter (Fig. 2D). To quantify this structural difference, we measured the diameter of >3000 follicles in PBF-Tg and WT mice at 26 weeks of age ($N = 5$ PBF-Tg and 7 WT mice; Fig.

2E). WT mice had an increased frequency of smaller diameter follicles of $<50 \mu\text{m}$ diameter ($P < 0.0001$ compared with PBF-Tg). In contrast, transgenic mice showed a greater preponderance of follicles which exceeded $50 \mu\text{m}$ diameter than WT ($50\text{-}100 \mu\text{m}$, $P = 0.0027$; $100\text{-}150 \mu\text{m}$, $P < 0.0001$; $150\text{-}200 \mu\text{m}$, $P = 0.0042$, $N = 12$, PBF-Tg v WT in each case). The mean follicle diameter in PBF-Tg mice ($81.3 \pm 0.2 \mu\text{m}$, $N = 1444$) was also greater compared with WT mice ($59.1 \pm 0.1 \mu\text{m}$, $N = 1759$, $P = 0.0002$). Thus, thyroids of PBF-Tg mice at 26 weeks of age are larger and heavier than matched WT litter-mates at least partially due to an increased frequency of large diameter follicles.

Thyroid-specific over-expression of PBF induces hyperplastic lesions

PBF has previously been shown to induce subcutaneous tumours in nude mice (8). We therefore examined thyroid morphology at 26, 52 and 78 weeks of age (Fig. 3 and Supplementary Fig. S5 and 6). PBF-Tg mice were prone to macrofollicular lesions, with $>65\%$ mice demonstrating macrofollicular lesions by 52 weeks of age, and $>90\%$ by 78 weeks ($P = 0.0217$ compared with WT, Fig. 3A and C and Supplementary Fig. S5). Macrofollicular lesions were also occasionally present in aging WT mice, but with lower frequency (Fig. 3A). Focal and nodular hyperplasia was also prominent, with 75% of PBF-Tg mice demonstrating evidence of hyperplastic lesions by 78 weeks of age (Fig. 3B, $P = 0.009$ compared with WT mice). Representative images of thyroid hyperplasia in 52 and 78 week old PBF-Tg mice are highlighted (Fig. 3D and F-I and Supplementary Fig. S6). Close examination of hyperplastic lesions also revealed the presence of larger nuclei (arrowed), a finding which is consistent with proliferating cells (Fig. 3H). In contrast, there were no hyperplastic lesions present in WT mice thyroids at any age (Fig. 3B and E). Whilst hyperplasia was prevalent in PBF-Tg mice there was no tumour induction, suggesting that although over-expression of PBF within murine thyroid follicular epithelial cells induces gross morphological changes and hyperplasia, it is insufficient alone to elicit cell transformation.

Thyroid function and gene expression responses to targeted PBF expression

We next investigated thyroid function in response to transgene expression in 6-7 week old PBF-Tg and WT mice by determining serum levels of total triiodothyronine (T3), thyroxine (T4) and TSH. Serum TSH levels were not elevated in either male or female PBF-Tg mice compared to sex-matched WT mice (Fig. 4A, $N = 6$ in each group). In addition, there was no significant difference between serum TSH levels in 12 month old PBF-Tg and WT mice (data not shown). In keeping with this, total T3 and T4 serum concentrations in PBF-Tg mice were not markedly altered compared with WT mice (Supplementary Fig. S7). These results indicate that PBF over-expression in the thyroid gland does not significantly alter thyroid function, resulting in increased serum TSH levels and hence stimulated thyroid cell growth.

To probe the mechanisms of induction of thyroid growth we next investigated growth factor and TSH receptor (TSHR) expression in PBF-Tg mice. Expression of mRNAs encoding VEGF, TGF β , EGF and IGF-1 was unaltered in PBF-Tg versus WT mice (Fig. 4B). Given that PBF has previously been implicated in the stimulation of FGF-2 expression by its binding partner PTTG, an unexpected finding was that FGF-2 showed a mild 25% reduction in expression in PBF-Tg mice ($P = 0.005$). In contrast, TSHR mRNA expression was significantly enhanced in PBF-Tg mice (2.0 ± 0.2 -fold, $P = 0.0002$). Additionally, TSHR mRNA was increased by 2.3 ± 0.4 -fold in primary thyrocyte cultures from PBF-Tg mice after 14-days of culture compared with WT ($P = 0.02$, $N = 8$; Fig. 4C). We next examined TSHR protein expression (Fig. 4D). Scanning densitometry confirmed that TSHR expression overall was significantly induced in PBF-Tg thyroids compared with matched WT mice (2.6 ± 0.4 -fold, $P = 0.021$).

Given that TSHR showed dysregulation, we next examined the mRNA expression of 4 further critical thyroid genes (Fig. 4E). Whilst PTTG has previously been shown to stimulate PBF expression *in vitro* (8), there was no reciprocal relationship *in vivo*, with PTTG mRNA expression unaffected by PBF over-expression (Fig. 4E). Thyroglobulin (Tg), thyroid transcription factor 1 (TTF1) and paired box gene 8 (PAX8) expression were also similar in PBF-Tg and WT mice. However, mRNA expression of the sodium iodide symporter NIS was repressed by ~50% in age and sex-matched PBF-Tg mice compared with WT (Fig. 4E, $P = 0.0004$). Assessment of NIS immunostaining in thyroid sections revealed a heterogeneity of NIS expression across whole thyroid lobes (Supplementary Fig. S8), but with an overall reduction in NIS protein expression in PBF-Tg mice compared to WT (Fig. 4F).

PBF represses sodium iodide symporter function *in vivo*

We have previously reported that PBF inhibits iodide uptake *in vitro* (2, 6). Given that PBF-Tg mice showed repressed NIS mRNA and protein expression, we examined NIS function in our transgenic mouse model. We thus performed primary cultures of thyroid cells from age and sex-matched PBF-Tg and WT mice, and performed ^{125}I uptake assays after 7 days of culture (Fig. 4G). Uptake was in the range of 3,000 to 13,000 cpm/ μg protein. Results corrected for protein concentration revealed a potent and significant ~70% repression of ^{125}I uptake in PBF-Tg mice compared with WT ($P = 0.0004$).

To determine whether the repression of radioiodide uptake – a critical issue in the treatment of benign and malignant thyroid disease – could be ameliorated, we transfected primary thyrocyte cultures from PBF-Tg mice with siRNA targeted to PBF. Following successful PBF knockdown (Fig. 4H), ^{125}I uptake increased 2.4 ± 0.64 -fold (Fig. 4I) to levels indistinguishable from WT ($P = 0.86$), whereas transfection using a scrambled siRNA did not alter ^{125}I uptake. Thus, our findings validate our previous *in vitro* reports that PBF represses NIS, demonstrating potent inhibition of NIS expression and function in thyroid cells *in vivo*. Furthermore, the repressed iodide uptake phenotype of PBF transgenic mice could be rescued by transiently down-regulating PBF expression.

PBF over-expression induces thyroid cell proliferation *in vivo*

Because thyroid cell growth is regulated by a series of well described kinase pathways which are frequently disrupted in neoplasia, we next investigated expression of proteins involved in the mitogen activated protein kinase (MAPK) and phosphoinositide 3-kinase (PI3K) pathway to understand how PBF might induce thyroid growth. Whilst MAPK was not altered in PBF-Tg mice compared with WT (Supplementary Fig. S9), phosphorylation of the PI3K target AKT (pAkt) was significantly induced by 3.2 ± 0.33 -fold (Fig. 5A, $N = 7$, $P = 0.00014$). In contrast, cellular expression of total Akt was unchanged (0.87 ± 0.08 -fold, $N = 8$, $P = 0.39$) in PBF-Tg mice. In support of this, Figure 5B shows that transient PBF over-expression in human thyrocytes similarly resulted in clear and significant activation of pAkt 24 hours post-transfection, whilst there was no difference in total AKT in human thyrocytes transfected with either vector only or pcDNA3-PBF.

We next assessed whether elevated pAkt might induce a downstream proliferative change by determining expression of the proliferative marker cyclin D1 in > 60,000 follicular epithelial cells from PBF-Tg and WT mice. Positive immunostaining with cyclin D1 was 2.7- to 3.4-fold greater in diffuse goitre regions of PBF-Tg mice by 52 ($P < 0.0001$) and 78 ($P = 0.00016$) weeks of age respectively compared to WT mice (Fig. 5C and D and Supplementary Fig. S10A). Taking the data as a whole, the mean percentage of cyclin D1 positive follicular epithelial cells in aged PBF-Tg mouse thyroid glands was 13.4% ($N = 4834/35958$ cells, $P < 0.0001$) compared with 4.7% in WT mice ($N = 1231/25987$ cells).

Further, hyperplastic regions of aged PBF-Tg mice demonstrated much greater cyclin D1 staining in follicular epithelial cells, ranging from 19% to 68%, with a mean value of $37.7 \pm 20.7\%$ (Fig. 5E and Supplementary Fig. S10B-D). Altogether, these results show that PBF over-expression results in increased thyroid cell proliferation *in vivo*, which is associated with activation of the Akt signalling pathway, as well as increased TSHR.

PBF and NIS expression and function in human MNG

PBF has previously been shown to be increased in differentiated thyroid cancer (8), but has not been examined in thyroid hyperplasia. Given that PBF induced goitre formation in our murine model, we next assessed PBF mRNA and protein expression in human MNG (Fig. 6). PBF mRNA was increased 2.2 ± 0.3 -fold, with scatter plot analysis showing that PBF mRNA expression was up to 5.6-fold higher in MNG than in normal thyroid (Fig. 6A). Protein expression was similarly induced in MNG compared with normal thyroid (2.3 ± 0.3 -fold, $P = 0.018$; Fig. 6B). We further assessed TSHR upregulation in MNG tissue samples. In direct support of our *in vitro* and *in vivo* data, human MNG tissue samples demonstrated a 4.5 ± 0.7 -fold increase in TSHR protein expression compared to normal tissue ($P = 0.003$; Fig. 6B).

In contrast to PBF and TSHR, NIS mRNA expression was significantly reduced in MNG (38% reduction, $P = 0.002$) compared with normal thyroid (Fig. 6C). Since we have shown in the PBF-Tg mouse that PBF reduces NIS expression, potential associations between these two genes in human MNG were examined. A significant negative correlation between PBF and NIS mRNA expression was apparent in MNG specimens (Fig. 6D, $r_s = 0.39$, $P = 0.05$).

Finally, to investigate whether over-expression of PBF in human thyroid hyperplasia and neoplasia might represent a therapeutic target, we performed primary culture of normal human thyrocytes, and investigated the outcome of manipulating PBF expression on radioiodide uptake. As in murine cultures, siRNA treatment resulted in repressed PBF expression in human thyrocytes (Fig. 6E), which was associated with a significant increase in NIS mRNA expression by 2.1 ± 0.35 -fold ($P = 0.02$) at 72 hours post-transfection (Fig. 6F). By contrast, there was no significant change in TSHR mRNA expression coincident with NIS upregulation (Supplementary Fig. S11). Crucially, however, in comparison to using scrambled siRNA, targeted repression of endogenous PBF expression in human thyrocytes was associated with a significant gain in radioiodide uptake by 2.0 ± 0.14 -fold (Fig. 6G, $P = 0.0001$).

Discussion

The mechanisms governing thyroid cell growth in hyperplasia and neoplasia remain to be fully defined, despite recent progress with well characterised oncogenes such as BRAF (21, 22). Our current study indicates that the relatively uncharacterised gene PBF should be considered a new aetiological factor in the thyroid, as well as a novel therapeutic target.

A possible role for PBF in tumourigenesis was highlighted by previous data showing that subcutaneous expression of murine fibroblasts over-expressing PBF induced high-grade malignant tumour formation in athymic nude mice (8). To gain insights into the wider role of PBF in thyroid disease, we constructed a PBF-Tg transgenic mouse model using the bovine thyroglobulin promoter to mediate thyroid-specific PBF over-expression. In contrast to our previous subcutaneous study, thyroid tumour induction was absent in this transgenic mouse model. Instead, transgenic mice demonstrated thyroid enlargement with 100% penetrance, with a high occurrence of both macrofollicular and hyperplastic thyroid lesions. Our findings are paralleled by observations from the $Pten^{L/L};TPO-Cre$ mouse model, in which there is constitutive activation of the PI3K/Akt pathway in thyrocytes, extremely

enlarged follicles and normal serum TSH concentrations (23). Hyperplasia and adenomas also developed in the Pten^{L/L};TPO-Cre mouse by 10 months of age, which was associated with an increase in thyrocyte proliferation (23). Thus, in concert with the Pten^{L/L};TPO-Cre mouse model, PBF-Tg mice demonstrate molecular hallmarks of altered cell number and morphology, evidenced by pAkt activation and increased cyclin D1 staining, but not tumours. It is likely therefore that cooperation between PBF-induced Akt signalling and mutations in other signalling cascades might be required to promote thyroid cancer pathogenesis. The precedent for this lies again with the Pten^{L/L};TPO-Cre mouse, which when crossed with mice harbouring a Kras oncogenic mutation led to invasive and metastatic follicular carcinomas (24), whereas neither the Pten^{L/L};TPO-Cre or Kras^{G12D} mouse model alone developed thyroid carcinomas.

PBF protein in our transgenic thyroids was induced 7-fold compared to endogenous mouse PBF expression, which was comparable to the highest fold increase in PBF expression in our MNG samples. Hence, the striking enlargement of PBF-Tg mouse thyroids was most likely the result of specific biological effects of PBF and not due to excessive exogenous protein expression. Primarily, the growth of thyroid cells is induced by TSH, which is in turn regulated by thyroid hormones through negative feedback at the anterior pituitary. Surprisingly, thyroid growth in the PBF-Tg mouse was not stimulated by elevated serum TSH levels. These results are in sharp contrast to the BRAF^{V600E} mouse which had similar enlargement of the thyroid gland but was associated with an 80-fold increase in TSH levels in 5-week old mice (22). Instead, gross enlargement of the PBF-Tg mouse thyroid was associated with increased TSHR expression and Akt activation. The precise mechanism by which PBF induces TSHR and Akt is the subject of further work, and it would be interesting in future long-term studies to place PBF-Tg mice on a thyroxine-supplemented diet to suppress TSH, thereby investigating the extent to which goitrogenesis is mediated via the TSH-TSHR axis.

Most activities of the TSHR are mediated through the G α s protein, which activates the adenylyl cyclase/cAMP cascade (25). Recent studies have also shown that TSH can stimulate Akt phosphorylation in rat FRTL5 (26) and PCCL3 cells (27, 28), presumably through coupling to G $\beta\gamma$ dimers and subsequent PI3K activation (28). These observations would suggest that PBF induction of TSHR might directly confer activation of PI3K/Akt signalling to promote thyroid cell proliferation *in vivo*. However, TSH effects on Akt phosphorylation have so far only been demonstrated *in vitro* (26-28) and so further investigations are required. It is possible that PBF over-expression might also activate Akt signalling independently of TSHR. Indeed, we recently observed that PBF over-expression can activate Akt in human colorectal HCT116 cells (unpublished observations).

The mechanism of PBF upregulation in human MNG is unknown. However, nodular thyroid disease is markedly more common in females than males (29), and we recently demonstrated in a separate study that PBF is oestrogen-regulated (11). PBF expression in transgenic PBF-Tg mice was under the control of the thyroglobulin promoter, and hence relatively immune to the effects of oestrogen. We did however observe significantly larger thyroid glands in female PBF-Tg mice compared to male littermates at 52 weeks of age, which might imply that oestrogen has a role in controlling PBF's ability to induce thyroid growth. Recently it was shown that circulating oestrogen can regulate thyroid cell proliferation in Pten^{L/L};TPO-Cre mice, but not in WT mice (30). These findings raise the possibility that PBF over-expression to activate PI3K/Akt signalling might be a contributory factor in increasing the susceptibility of females to thyroid disease. It would therefore be interesting to compare oestrogen status and PBF expression in a large series of human MNG, as well as male versus female PBF expression in thyroid disease in general.

Radioiodine is central to the treatment of thyroid cancer and toxic nodular hyperthyroidism. It is also increasingly used as first line therapy in Graves' disease (31) and to induce shrinkage of benign goitres (32). Our murine data provide an important validation of our earlier *in vitro* observations that PBF is a critical regulator of both NIS expression and function (2, 6). Mice with targeted over-expression of PBF demonstrated a 70% repression of iodide uptake in primary thyroid cultures. As we observed a ~50% inhibition of NIS mRNA expression in PBF-Tg thyroids compared to WT controls, repressed iodide uptake in PBF-Tg mice cultures may also reflect altered subcellular localisation of NIS (6). Whilst two recent studies have implicated PI3K/Akt signalling in NIS inhibition (28, 33), the exact mechanism for PBF-induced NIS mRNA repression remains to be fully clarified.

In MNG, NIS expression is heterogeneous, but is generally increased in hyperfunctioning goitres and low in those that are non-toxic (34-37). Our data of reduced NIS expression in MNG are therefore in keeping with those in the literature. Indeed, the observed phenotype is similar to that of cold thyroid nodules that have reduced NIS mRNA levels and show reduced iodide uptake on scintiscan (35). Importantly, we were able to demonstrate a significant correlation between PBF and NIS mRNA expression in MNG, which further emphasises the functional interaction between these two genes *in vivo*. In addition, we were able to demonstrate that NIS expression was heterogeneous throughout the thyroid lobes of PBF-Tg mice, mirroring the typical non-uniformity of radioiodine uptake in human MNG. It will be important to investigate in future studies whether specific regions of high PBF expression in human MNG represent thyroidal regions of lowered radioiodine uptake.

Of central importance to the current investigation is the observation that we were able to rescue NIS repression by siRNA targeting of PBF both in primary thyroid cultures from transgenic mice and in normal human thyrocytes. The functional interaction between PBF and NIS was further demonstrated by a significant 2-fold increase in NIS mRNA expression following siRNA targeting of PBF in primary human thyrocytes. These results therefore suggest that PBF represents a promising and novel therapeutic target to overcome radioiodine resistance in thyroid tumours and their metastases, as well as in thyroid disease more generally.

In summary, we present evidence that the relatively uncharacterised proto-oncogene PBF has specific relevance to thyroid cell growth. As well as inducing thyroid cell proliferation and hence goitre *in vivo*, PBF represses the central therapeutic avenue for thyroid hyperplasia and neoplasia. Thus, in addition to its established role in thyroid cancer, PBF now needs to be further appraised as a critical gene in the aetiology and treatment of thyroid disease as a whole.

Supplementary Material

Refer to Web version on PubMed Central for supplementary material.

Acknowledgments

We thank Andrea Bacon, Laurence Loubiere, Ann Logan and Anna Maria Gonzalez for technical help. This work was supported by grants from the Get-Ahead Charity, the Medical Research Council and the Wellcome Trust.

References

1. Boelaert K, Tannahill LA, Bulmer JN, Kachilele S, Chan SY, Kim D, et al. A potential role for PTTG/securin in the developing human fetal brain. *Faseb J*. 2003; 17:1631–9. [PubMed: 12958169]
2. Boelaert K, Smith VE, Stratford AL, Kogai T, Tannahill LA, Watkinson JC, et al. PTTG and PBF repress the human sodium iodide symporter. *Oncogene*. 2007; 26:4344–56. [PubMed: 17297475]

3. Chien W, Pei L. A novel binding factor facilitates nuclear translocation and transcriptional activation function of the pituitary tumor-transforming gene product. *J Biol Chem.* 2000; 275:19422–7. [PubMed: 10781616]
4. Mo Z, Zu X, Xie Z, Li W, Ning H, Jiang Y, et al. Antitumor effect of F-PBF(beta-TrCP)-induced targeted PTTG1 degradation in HeLa cells. *J Biotechnol.* 2009; 139:6–11. [PubMed: 18977400]
5. Reynolds LE, Watson AR, Baker M, Jones TA, D'Amico G, Robinson SD, et al. Tumour angiogenesis is reduced in the Tc1 mouse model of Down's syndrome. *Nature.* 2010; 465:813–7. [PubMed: 20535211]
6. Smith VE, Read ML, Turnell AS, Watkins RJ, Watkinson JC, Lewy GD, et al. A novel mechanism of sodium iodide symporter repression in differentiated thyroid cancer. *J Cell Sci.* 2009; 122:3393–402. [PubMed: 19706688]
7. Stock M, Schafer H, Fliegau M, Otto F. Identification of novel genes of the bone-specific transcription factor Runx2. *J Bone Miner Res.* 2004; 19:959–72. [PubMed: 15190888]
8. Stratford AL, Boelaert K, Tannahill LA, Kim DS, Warfield A, Eggo MC, et al. Pituitary tumor transforming gene binding factor: a novel transforming gene in thyroid tumorigenesis. *J Clin Endocrinol Metab.* 2005; 90:4341–9. [PubMed: 15886233]
9. Tfelt-Hansen J, Yano S, Bandyopadhyay S, Carroll R, Brown EM, Chattopadhyay N. Expression of pituitary tumor transforming gene (PTTG) and its binding protein in human astrocytes and astrocytoma cells: function and regulation of PTTG in U87 astrocytoma cells. *Endocrinology.* 2004; 145:4222–31. [PubMed: 15178645]
10. Yaspo ML, Aaltonen J, Horelli-Kuitunen N, Peltonen L, Lehrach H. Cloning of a novel human putative type Ia integral membrane protein mapping to 21q22.3. *Genomics.* 1998; 49:133–6. [PubMed: 9570958]
11. Watkins RJ, Read ML, Smith VE, Sharma N, Reynolds GM, Buckley L, et al. Pituitary tumor transforming gene binding factor: a new gene in breast cancer. *Cancer Res.* 2010; 70:3739–49. [PubMed: 20406982]
12. Bork P, Doerks T, Springer TA, Snel B. Domains in plexins: links to integrins and transcription factors. *Trends Biochem Sci.* 1999; 24:261–3. [PubMed: 10390613]
13. Bacon A, Kerr NC, Holmes FE, Gaston K, Wynick D. Characterization of an enhancer region of the galanin gene that directs expression to the dorsal root ganglion and confers responsiveness to axotomy. *J Neurosci.* 2007; 27:6573–80. [PubMed: 17567818]
14. Hogan, B.; Beddington, R.; Costantini, F.; Lacey, E. *Manipulating the mouse embryo.* Cold Spring Harbour Laboratory; New York: 1994.
15. Ballester M, Castello A, Ibanez E, Sanchez A, Folch JM. Real-time quantitative PCR-based system for determining transgene copy number in transgenic animals. *Biotechniques.* 2004; 37:610–3. [PubMed: 15517974]
16. Read ML, Mir S, Spice R, Seabright RJ, Suggate EL, Ahmed Z, et al. Profiling RNA interference (RNAi)-mediated toxicity in neural cultures for effective short interfering RNA design. *J Gene Med.* 2009; 11:523–34. [PubMed: 19322910]
17. Kim D, Pemberton H, Stratford AL, Buelaert K, Watkinson JC, Lopes V, et al. Pituitary tumour transforming gene (PTTG) induces genetic instability in thyroid cells. *Oncogene.* 2005; 24:4861–6. [PubMed: 15897900]
18. Clarke WE, Berry M, Smith C, Kent A, Logan A. Coordination of fibroblast growth factor receptor 1 (FGFR1) and fibroblast growth factor-2 (FGF-2) trafficking to nuclei of reactive astrocytes around cerebral lesions in adult rats. *Mol Cell Neurosci.* 2001; 17:17–30. [PubMed: 11161466]
19. Jeker LT, Hejazi M, Burek CL, Rose NR, Caturegli P. Mouse thyroid primary culture. *Biochem Biophys Res Commun.* 1999; 257:511–5. [PubMed: 10198242]
20. Pohlenz J, Weiss RE, Cua K, Van Sande J, Refetoff S. Improved radioimmunoassay for measurement of mouse thyrotropin in serum: Strain differences in thyrotropin concentration and thyrotroph sensitivity to thyroid hormone. *Thyroid.* 1999; 9:1265–71. [PubMed: 10646670]
21. Franco AT, Malaguarnera R, Refetoff S, Liao XH, Lundsmith E, Kimura S, et al. Thyrotrophin receptor signaling dependence of Braf-induced thyroid tumor initiation in mice. *Proc Natl Acad Sci U S A.* 2011; 108:1615–20. [PubMed: 21220306]

22. Knauf JA, Ma X, Smith EP, Zhang L, Mitsutake N, Liao XH, et al. Targeted expression of BRAFV600E in thyroid cells of transgenic mice results in papillary thyroid cancers that undergo dedifferentiation. *Cancer Res.* 2005; 65:4238–45. [PubMed: 15899815]
23. Yeager N, Klein-Szanto A, Kimura S, Di Cristofano A. Pten loss in the mouse thyroid causes goiter and follicular adenomas: insights into thyroid function and Cowden disease pathogenesis. *Cancer Res.* 2007; 67:959–66. [PubMed: 17283127]
24. Miller KA, Yeager N, Baker K, Liao XH, Refetoff S, Di Cristofano A. Oncogenic Kras requires simultaneous PI3K signaling to induce ERK activation and transform thyroid epithelial cells in vivo. *Cancer Res.* 2009; 69:3689–94. [PubMed: 19351816]
25. Vassart G, Dumont JE. The thyrotropin receptor and the regulation of thyrocyte function and growth. *Endocr Rev.* 1992; 13:596–611. [PubMed: 1425489]
26. Morshed SA, Latif R, Davies TF. Characterization of thyrotropin receptor antibody-induced signaling cascades. *Endocrinology.* 2009; 150:519–29. [PubMed: 18719020]
27. de Souza EC, Padron AS, Braga WM, de Andrade BM, Vaisman M, Nasciutti LE, et al. MTOR downregulates iodide uptake in thyrocytes. *J Endocrinol.* 2010; 206:113–20. [PubMed: 20392814]
28. Zaballos MA, Garcia B, Santisteban P. Gbetagamma dimers released in response to thyrotropin activate phosphoinositide 3-kinase and regulate gene expression in thyroid cells. *Mol Endocrinol.* 2008; 22:1183–99. [PubMed: 18202153]
29. Tonacchera M, Pinchera A, Vitti P. Assessment of nodular goitre. *Best Pract Res Clin Endocrinol Metab.* 2010; 24:51–61. [PubMed: 20172470]
30. Antico-Arciuch VG, Dima M, Liao XH, Refetoff S, Di Cristofano A. Cross-talk between PI3K and estrogen in the mouse thyroid predisposes to the development of follicular carcinomas with a higher incidence in females. *Oncogene.* 2010; 29:5678–86. [PubMed: 20676139]
31. Weetman AP. Radioiodine treatment for benign thyroid diseases. *Clin Endocrinol (Oxf).* 2007; 66:757–64. [PubMed: 17466000]
32. Hegedus L, Bonnema SJ, Bennedbaek FN. Management of simple nodular goiter: current status and future perspectives. *Endocr Rev.* 2003; 24:102–32. [PubMed: 12588812]
33. Kogai T, Sajid-Crockett S, Newmarch LS, Liu YY, Brent GA. Phosphoinositide-3-kinase inhibition induces sodium/iodide symporter expression in rat thyroid cells and human papillary thyroid cancer cells. *J Endocrinol.* 2008; 199:243–52. [PubMed: 18762555]
34. Joba W, Spitzweg C, Schriever K, Heufelder AE. Analysis of human sodium/iodide symporter, thyroid transcription factor-1, and paired-box-protein-8 gene expression in benign thyroid diseases. *Thyroid.* 1999; 9:455–66. [PubMed: 10365677]
35. Krohn K, Fuhrer D, Bayer Y, Eszlinger M, Brauer V, Neumann S, et al. Molecular pathogenesis of euthyroid and toxic multinodular goiter. *Endocr Rev.* 2005; 26:504–24. [PubMed: 15615818]
36. Lazar V, Bidart JM, Caillou B, Mahe C, Lacroix L, Filetti S, et al. Expression of the Na⁺/I⁻ symporter gene in human thyroid tumors: a comparison study with other thyroid-specific genes. *J Clin Endocrinol Metab.* 1999; 84:3228–34. [PubMed: 10487692]
37. Russo D, Bulotta S, Bruno R, Arturi F, Giannasio P, Derwahl M, et al. Sodium/iodide symporter (NIS) and pendrin are expressed differently in hot and cold nodules of thyroid toxic multinodular goiter. *Eur J Endocrinol.* 2001; 145:591–7. [PubMed: 11720877]

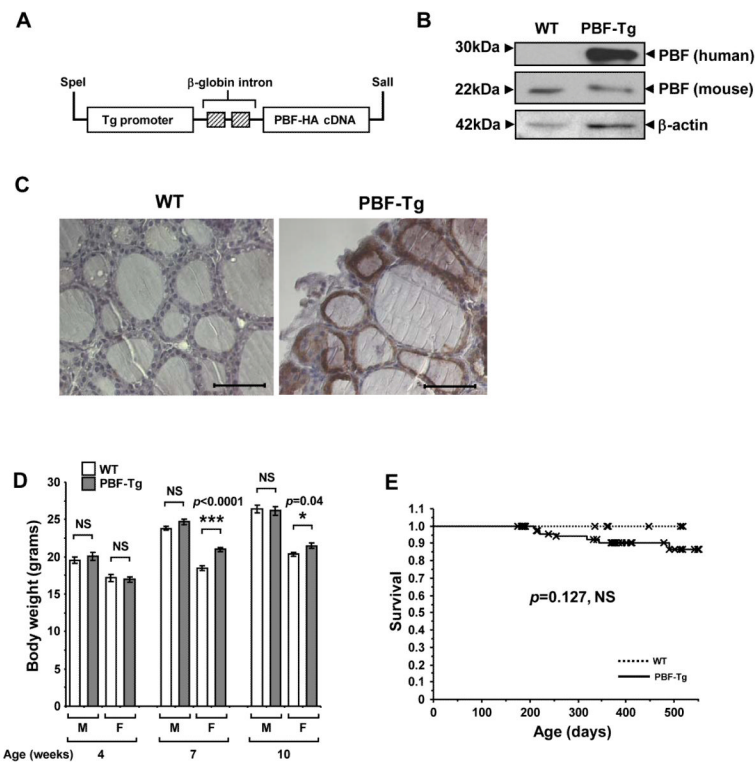


Figure 1. Generation and characterisation of the PBF-Tg mouse model. A, Schematic of the bovine thyroglobulin (Tg)-PBF-HA transgene. B, Detection of transgenic PBF (human) and endogenous PBF (mouse) expression by Western blot analysis of PBF-Tg and WT thyroids. C, Detection of HA-tagged PBF (brown staining) by immunohistochemistry in PBF-Tg and WT thyroid sections. Scale bars: 50 μ m. D, Body weight of male (M) and female (F) PBF-Tg and WT mice at 4, 7 and 10 weeks of age ($N = 7-45$). Data presented as mean \pm SE. E, Kaplan-Meier survival curves for PBF-Tg ($N = 82$) and WT ($N = 31$) mice; $P = 0.127$.

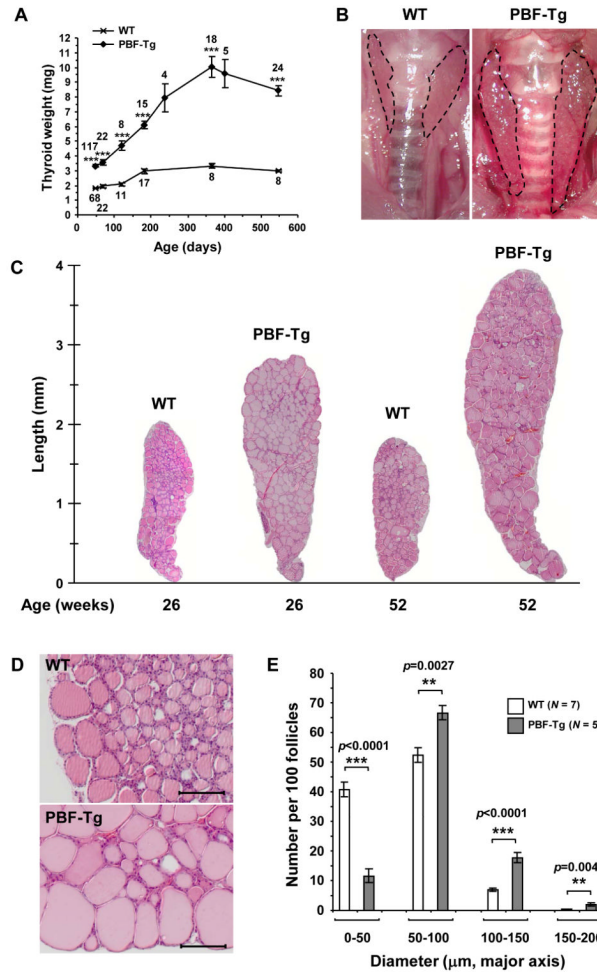


Figure 2. Enlarged thyroid glands in PBF-Tg mice. A, Thyroid weight of PBF-Tg and WT mice. $***P < 0.0001$ compared to age-matched WT mice. Mice numbers analysed are shown. B, Representative images of thyroid glands from 52-week old PBF-Tg and WT mice. Dotted line indicates margin of thyroid lobes. C, Representative images of H&E stained thyroid sections from PBF-Tg and WT mice at 26 and 52 weeks of age. D, Higher magnification of H&E stained sections of PBF-Tg and WT thyroids from 26 week old mice. Scale bars: 100 μm . E, Quantification of follicle diameter in PBF-Tg and WT thyroids from 26 week old mice expressed as frequency per 100 follicles measured. Data presented as mean \pm SE.

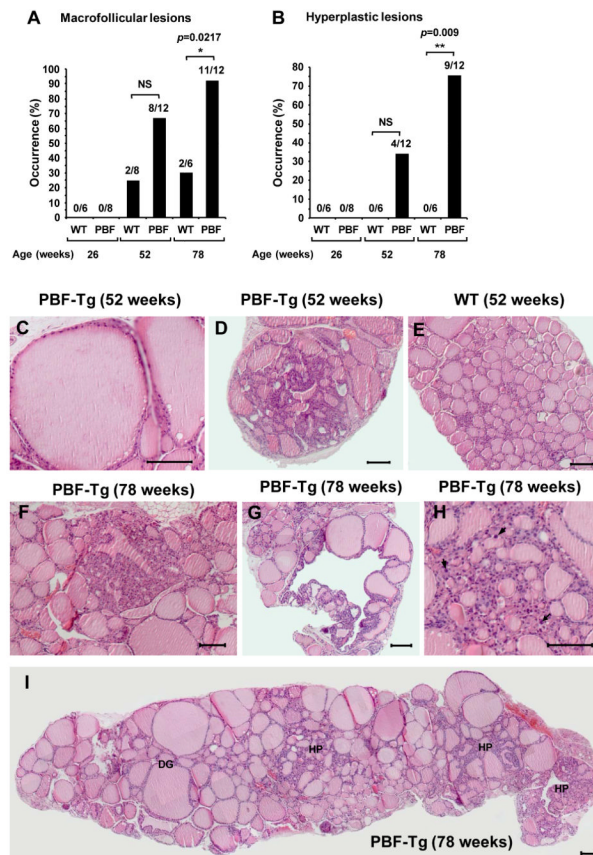
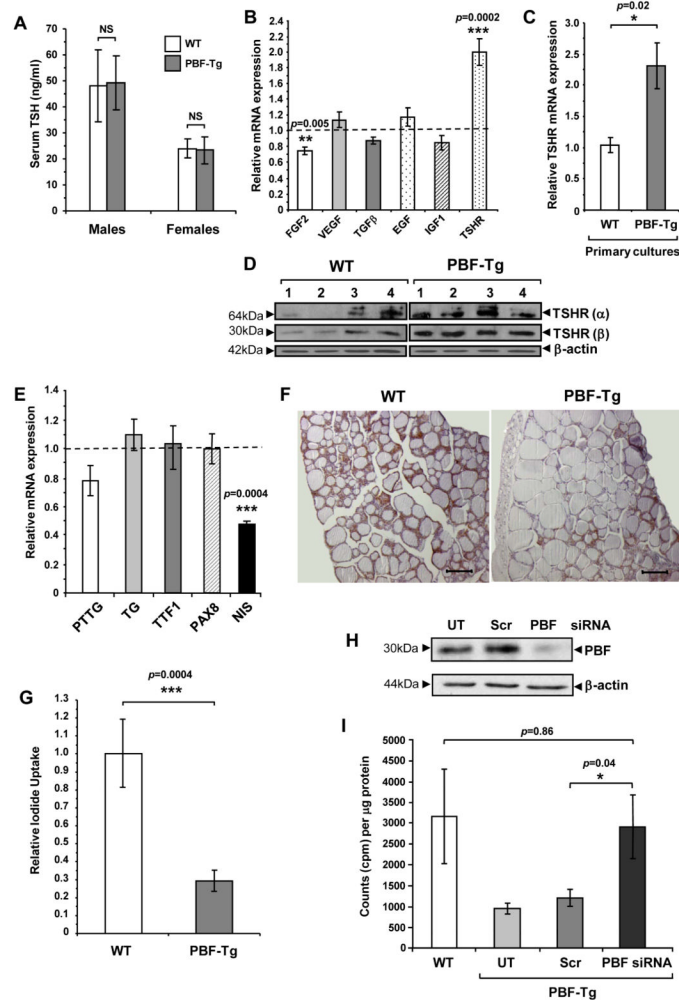
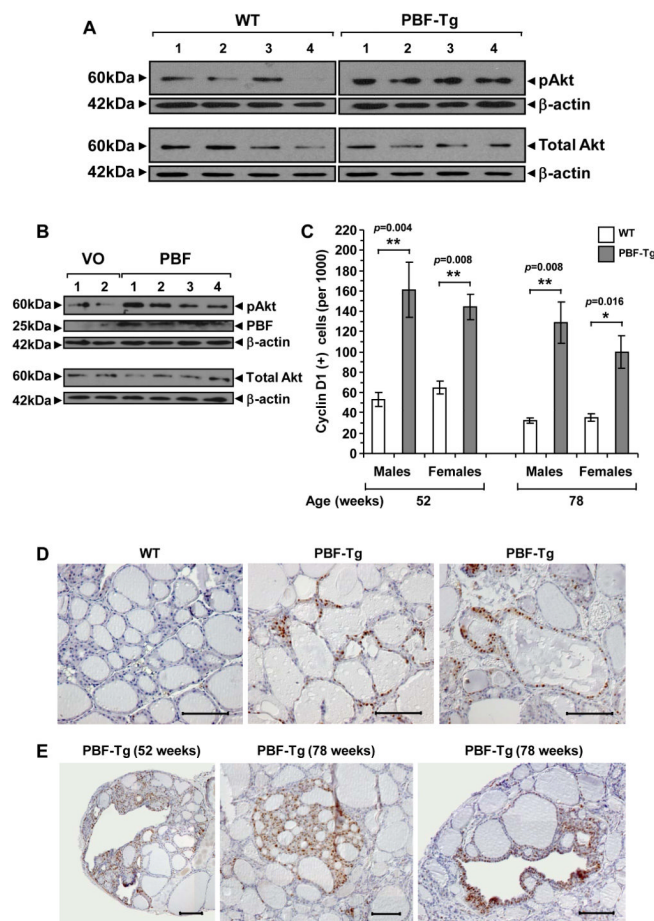


Figure 3.

Thyroid hyperplasia in PBF-Tg mice. Occurrence of macrofollicular (A) and hyperplastic lesions (B) in at least ten independent sectional planes per PBF-Tg or WT thyroid; $N = 6-12$ per genotype. Statistics analysed using Fisher's exact test. C-E, Representative H&E stained images of a macrofollicular lesion (C) and nodular hyperplasia (D) in PBF-Tg thyroids, and of a WT thyroid (E) in 52 week old mice. F-G, Representative H&E stained images of hyperplasia in PBF-Tg thyroids in 78 week old mice. H, Arrows highlight enlarged nuclei in the hyperplastic lesion. I, Composite image of an entire thyroid lobe from a 78 week old PBF-Tg mouse with diffuse goitre (DG) and hyperplastic regions (HP). Scale bars: 100 μm .

**Figure 4.**

Altered gene expression and iodide uptake in PBF-Tg thyroids. A, Serum TSH analyses in 6-week old PBF-Tg and WT mice; $N=6$. Relative mRNA expression of indicated growth factor and TSHR in either PBF-Tg thyroids (B) or primary thyrocyte cultures (C) compared to WT; $N=6-15$. D, Detection of TSHR isoforms α and β by Western blot analyses in PBF-Tg and WT thyroids; $N=4$. E, Relative mRNA expression of PTTG, TG, TTF1, PAX8 and NIS in PBF-Tg thyroids compared to WT; $N=6-13$. F, Detection of NIS by immunohistochemistry of PBF-Tg and WT thyroids. Scale bars: 100 μm . G, Relative ^{125}I uptake in primary thyrocyte cultures from PBF-Tg and WT mice; $N=5-6$. Detection of PBF-HA expression by Western blot analyses (H) and relative ^{125}I uptake (I) in primary PBF-Tg thyrocyte cultures either non-transfected (UT) or transfected with PBF and scrambled (Scr) siRNA as indicated; $N=8-20$. Data presented as mean \pm SE

**Figure 5.**

Cellular proliferation in PBF-Tg thyroids. A, Detection of pAkt and total Akt expression by Western blot analysis of PBF-Tg and WT thyroids. B, Detection of pAkt, total Akt and PBF by Western blot analysis of human thyrocytes transfected with either vector only (VO) or pcDNA3-PBF (PBF). C, Quantification of cyclin D1 immunostaining in sex- and age-matched PBF-Tg and WT thyroids, expressed as frequency of cyclin D1 positive cells per 1000 cells examined; $N = 5062-12998$ per thyroid. A total of 62,945 thyroid cells were examined for cyclin D1 expression in 17 PBF-Tg and 13 WT thyroids. Data presented as mean \pm SE. Representative images of cyclin D1 staining in diffuse goitre regions (D) and hyperplastic lesions (E) of PBF-Tg and WT thyroids are shown. Scale bars: 100 μ m.

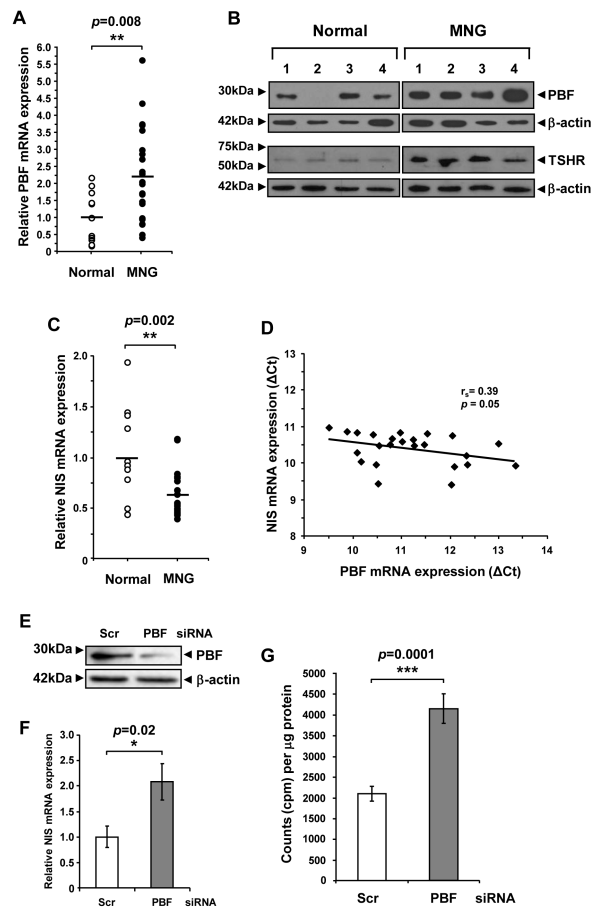


Figure 6.

Functional interaction between PBF and NIS in human thyrocytes. A, Quantification of PBF mRNA expression in MNG ($N=24$) relative to normal thyroid ($N=11$). Data presented as a scatterplot. B, Detection of PBF and TSHR expression by Western blot analyses in MNG and normal thyroids. C, Quantification of NIS mRNA expression in MNG ($N=24$) relative to normal thyroid ($N=11$). Data presented as a scatterplot. D, Correlation of PBF and NIS mRNA expression (shown as ΔCT values) in MNG and normal thyroid. Statistics analysed using Spearman rank correlation. E-G, Detection of PBF expression by Western blot analyses (E), quantification of NIS mRNA expression (F) and relative ^{125}I uptake (G) in primary human thyrocyte cultures transfected with either PBF or Scr siRNA as indicated; $N=9-11$. Data presented as mean \pm SE.